Construction and Building Materials 190 (2018) 349–362

Contents lists available at ScienceDirect

Construction and Building Materials

journal homepage: www.elsevier.com/locate/conbuildmat

Thermal decomposition of the CaO in traditional lime kilns. Applications in cultural heritage conservation

Esther Ontiveros-Ortega [a,*], Encarnación M. Ruiz-Agudo [b], Alfonso Ontiveros-Ortega [c,d]

[a] Andalusian Historical Heritage Institute (IAPH), Geology Laboratory (Spain), Avda. de Los Descubrimientos S/N, 41092 Sevilla, Spain
[b] Department of Mineralogy and Petrology I, University of Granada, 18071 Granada, Spain
[c] Department of Physics, University of Jaén (Spain), Campus Universitario de las Lagunillas s/n, edificio A-3, 23071 Jaén, Spain
[d] Instituto Andaluz de Geofísica, University of Granada, Fuentenueva s/n, 18002 Granada, Spain

HIGHLIGHTS

- The calcination process of the limestones depends of the porosity and crystalline structure original of the limestones.
- The calcination temperatures, longer residence time and CO_2 and steam pressure affects the size and porosity of the CaO crystals.
- The quicklimes calcined in traditional kilns are characterized by greater particle and pore size.
- The quicklimes with greater volume of pores, the lime slaking reaction is less exothermic.
- The size of the particles CaO affects the rate of the lime slaking reaction.

ARTICLE INFO

Article history:
Received 10 April 2018
Received in revised form 20 August 2018
Accepted 11 September 2018
Available online 27 September 2018

Keywords:
Limestone
Lime
Quicklime
Calcination process
Traditional lime kilns
Industrial lime kilns
Porosity
Particle size

ABSTRACT

It has been the aim of this paper to know the factors that most affect to the process of obtaining the quicklime in traditional lime kilns. To this end, a comparative study has been carried out between two quicklime types, one obtained in traditional lime kiln and another obtained in an industrial lime kiln. On the other hand, two limestone types, commonly used in the production of lime in these kilns, have been calcination in the laboratory. They correspond to an oosparite and oomicritic limestones, traditionally used in the elaboration of limes in the *Morón de la Frontera* region, Seville (Spain). The samples have been analyzed from the chemical, physical and mineralogical points of view. The calcination process of the limestones and the optimum heating temperature depends of the porosity and crystalline structure original of the limestones. The calcination temperatures, longer residence time and CO_2 and steam pressure in the kilns affects the size and porosity of the CaO crystals. The quicklimes with greater volume of pores allow faster access of water to the interior of the material and consequently the lime slaking reaction is less exothermic. The size of the particles CaO affects the rate of the lime slaking reaction, accelerating the reaction when the particles are smaller. The quicklimes calcined in traditional kilns are characterized by greater particle and pore size and greater volume of mesopores.

1. Introduction

Traditional and semi-industrialized products based on lime, constitute a proposal that has been growing in recent years. Their use as restoration material for conservation of historic buildings it highlights in this paper, based on its compatibility with this type of construction materials [1,2]. However, lime is a material of interest for other industrial applications such as food processing, disinfection, water treatment, SO_2 post-combustion capture, steel-making, plastics, glass, sugar refining and agriculture. Currently other applications of interest are emerging that shows a potential use in the future as stabilizer of demolition materials, such as crushed brick and crushed concrete pavement, for your application in road construction [3,4]. In all cases, its environmental interest is highlighted by reducing the emission of CO_2 into the atmosphere.

Lime is a material obtained through a group of processes that are include within the term *lime cycle*. This cycle includes a first stage of calcination of limestone between 850 and 900 °C to obtain quicklime (CaO). During the calcination process, quicklime and carbon dioxide are produced according to the reaction (1)

$$CaCO_3 + \Delta H_R \leftrightarrow CaO + CO_2 \uparrow \quad (1)$$

* Corresponding author.
E-mail address: esther.ontiveros@juntadeandalucia.es (E. Ontiveros-Ortega).

https://doi.org/10.1016/j.conbuildmat.2018.09.059
0950-0618/

where ΔH_R corresponds to reaction enthalpy. This reaction reaches equilibrium when the Pco_2 equals the equilibrium constant (Keq); therefore, the lower Pco_2 favors calcination of the limestone.

Heat is transferred from outside to inside of limestone by thermal conductivity and the heat transfer velocity through the lime, already formed; it becomes increasingly slow until reach entire calcination of the limestone.

The understanding of kinetic of thermal decarbonation of calcium carbonate and reaction mechanism has been the object of many studies over the years. However, there are many aspects about the calcination reaction not well understood, and therefore there is no consensus about several fundamental aspects of the calcination process as particle reaction model, rate-limiting processes, and influence of the CO_2 partial and total pressure on the reaction rate [5].

A vast number of studies may be found in the literature with the goal to know the factors that control the decarbonation process of the limestones [6–22]. Several investigations have shown that the decomposition of the calcium carbonate occurs at a definite boundary between the CaCO3 and CaO phases, which moves at a constant rate towards the centre of the particle [23]. This involves the collapse of the crystal structure of calcite [24] and the formation of nanometric crystals of CaO [18].

The calcination or decarbonation process of the limestone takes place in several phases. At first heat transmission to the surface of the particle not calcined by convection and radiation takes place, subsequently the conduction of the heat through the already dissociated layer (CaO) to the reaction zone it is followed by the decomposition of carbonates on the reaction surface with the formation of calcium oxide and carbon dioxide and finally the diffusion of carbon dioxide from the porous layer of calcium oxide to the external surface of the particles and output of CO_2 to the atmosphere of kiln [25].

The transformation of calcite to CaO starts at 600 °C from outside to inside of rock and ends at 850 °C [8]. Three transformation mechanics control the process of decarbonation: the chemical decomposition, structural transformation and physical desorption. These mechanisms are controlled by the pressure of CO_2 and the temperature. The decarbonation of calcium carbonate can take place at a lower temperature if the CO_2 pressure in the kiln is lower than the partial dissociation pressure inside the material, at 1 atm of pressure the reaction takes place between 800 and 850 °C. In condition of equilibrium of partial pressure of CO_2; the reaction begins after a period of induction through areas of calcium carbonate with crystalline defects, which favors the diffusion of CO_2 to the outside. This explains the incidence of the crystallinity in the velocity of process [26].

The rate of decarbonation process can be limited by temperature, which controls the transfer of heat through the particle to the reaction interface. Also influence the velocity of the reaction that depends on the transfer of CO_2 released through the porous system and the chemical reaction [5].

If decarbonation takes place under conditions of low pressure of CO_2, the dominant mechanism is the chemical reaction, since the exhaust to the outside of CO_2 is rapid and the physical desorption can be ruled out for calcination under vacuum or at low pressures, in these conditions decarbonation is faster [18]. On the other hand, if the decarbonation takes place under conditions of high pressures of CO_2, according to the Fick diffusion, the escape of CO_2 through the metastable structure would be hindered and the rate of decarbonation decreases at least at low temperatures [26], increasing the possibility of recarbonatation of lime.

In the first case (low pressure of CO_2), the dominant mechanism for the growth of the CaO crystal would be the reticular diffusion and non-aggregation of particles; which is favored by an increase in temperature. If the conditions are of high temperature, smaller crystals are formed. In the second case (high pressures of CO_2), the dominant mechanism for crystal growth is particle agglomeration and subsequent sintering [18,26].

The microtextural characteristics of the limestone also have an important incidence in the process of calcination. In ancient architectural treatises was mentioned that the limestones rich in calcium carbonate [27], compact [28–32] and pure [33–35] were the most suitable because they generate more plastic lime putty [36]. Moreover, affects other factors such as the crystal structure. The differences in the crystallinity of the limestone and porosity seem to be an important factor, in the process of decarbonation [5,26]. The shape of crystals of CaO determines the intercrystalline porosity; larger pores allows easy to passage for CO_2 gases during calcination. The escape of these gases is important because they can affect the carbonated process; the CO_2 does not react with quicklime at ordinary atmospheric temperatures, but if the temperature increases, the carbonated starts slowly at 290 °C, increasing at 400 °C and acquiring great affinity at 600 °C [37]. On the other hand, lime impurities (SiO_2, Al_2O_3, Fe_2O_3) during the calcination process can generate cement clinker minerals, especially if the temperature is very high, further reducing the calcium content available for the reaction with water [26,38].

Hydrated lime also has important applications and its use also is millennial. Calcium hydroxide is an important chemical with numerous chemical, industrial, environmental, and architectural applications. Heterogeneous phase precipitation of Ca (OH)2 occurs following hydration of quicklime, a process known as *lime slaking*. The slaking process takes place according to the reaction (2)

$$CaO + H_2O \rightarrow Ca(OH)_2 + 15,300\ cal/grmol. \quad (2)$$

Quicklime slaking process depends of the conditions of calcination of the limestone [25,42], the temperature, surface area and size of the CaO particles are the factors that most affect.

The $Ca(OH)_2$ is a strong base where $[Ca^{+2}]$ and $[OH^-]$ are practically dissociated. The velocity of hydration process is controlled by the CaO solubility that favors the highest concentration of Ca^{+2} and OH^- ions. Another factor that affects is the pH, since the higher concentration of H^+ ions favors the solubility of CaO. On the other hand the greater reactivity of the lime is given by the size of the CaO crystals and its porosity, the velocity of CaO hydration is important because it directly affects the size of the portlandite crystals, $Ca(OH)_2$, a slow reaction generates smaller crystals [25]. These aspects, as we have seen previously, depend on the conditions of the calcination process of the limestone [26,39].

Based on this background; most of the works carried out have focused to the effect of the temperature and partial pressure of CO_2 on the properties acquired the quicklime, and more recently has been studied related aspects with micro-textural changes (surface area, porosity, crystallization, etc.) during the calcination process.

It is known that the chemical and physical properties of limestones and the quicklimes; such as the conductivity, mass transfer coefficient and diffusivity influence in the calcination process [40]. The calcination process of the limestones in the laboratory can be controlled, although hardly reproduce the conditions of a traditional lime kiln, so a microtextural analysis of these CaO can reveal interesting aspects about the production technology that characterize this type of kilns. Currently there are few works focused on the microtextural characteristics of the CaO generated in traditional lime kilns, so this work is of interest for the advancement of research in this field.

2. Material and methods

2.1. Lime production process

Traditional lime Kiln studied in this paper is of Arabic type (Fig. 1a) fed by combustible vegetation of olive and pine. These kilns operate with a volume of stone about 70 tons; with calcination times from 10 to 20 days, with continuous feed every 15 min and a substantial daily consumption of wood. Temperatures reached inside the kiln vary from 1100 °C, at the heat source, to 750 °C, in outer areas, with heat loss of 50 °C. Smoke color, from black to white, and change in color of the stone, from reddish orange to yellow-gold observed in the upper recesses of the kiln (caños o troneras) (see Fig. 1b), facilitate the determination of the exact heating of the stone. In the first hours of the kiln a white smoke escapes, because the stones gave off all the humidity, as the temperature increased the stones appear whitish and when the total evaporation of the water took place the smoke acquires a black hue, indicating that the kiln has reached the optimum temperature (850–1000 °C) necessary for the calcination [41].

The thermal decomposition of limestone in traditional lime kilns is characterized by an environment of not very high temperature but longer residence time. When wood is used, a heat is radiated through the kiln and although it does not reach high values, the heat is homogeneous; which makes the lime remain most porous, favoring the calcination complete of the stone [33]. It is also important to control the escape of CO_2 outside the kiln, the fuel consumption that depended on the type of stone, architectural characteristics of the kiln and atmospheric conditions [42]. In this type of kilns, subjected to more thermal stress due to the higher concentration of steam, quicklime more porous are generated [8]. The calcination process with steam can occur at a lower temperature, but it needs longer residence time. The steam reduces the energy requirement of decarbonation process, which may partially offset the energy required to produce the additional steam [21].

The kiln assembly is critical to the quality of the lime produced, because it is designed so that the temperature to which the stone is subjected inside is as homogeneous as possible. The assembly of vaults of the kiln and its structure (*Ahornado* process) is done via the method of dry stone, built with *armaderas* (larger stones) in a concentric arrangement (see Fig. 1c). These stones are fit with other smaller stones called *matacanes* and, finally, the gaps are filled with other small stones called *ripios* [41]. This design allows that temperature inside the kiln to be as homogeneous as possible. A wide range of particle size distribution in constructive design of the kiln also has an effect in distribution of heat inside. The small stones accumulate between the voids formed by large stones, thus impeding the draft and the flow of combustion flame and gases [43].

Industrial lime kilns used in this paper are continuous vertical type; fed with combustible natural, gas, coke, fuel and oil. Limestone is subjected to temperatures between 900 and 1000 °C over short periods of time; obtaining quicklime that is then sieved, crushed or ground and finally hydrated to obtain a very fine dry powder (powder lime).

2.2. Analyzed samples

It carried out a comparative study between three types of quicklimes (see Table 1). Two of these were obtained from the same limestones, but with different manufacturing technologies: CaO (TL) from traditional vertical kilns and CaO(IL) from industrial vertical kilns. On the other hand it has been analyzed a CaO(PL) of analytical purity supplied by Panréac (*ref: 211234.1211; lot: 0000534420 M = 56.08 g/mol)*.

Traditional Kilns are characterized by a heterogeneous burning, for this reason within the CaO (TL) two varieties were analyzed, located in different areas of the kiln with different calcination temperatures: CaO(TL1) at 1100 °C and CaO(TL2) at 900 °C. This was done to see as the temperature changes affected to physical properties and slaking kinetic.

On the other hand, it analyzed limestone used in the production of quicklime, concretely, two varieties extracted from two quarries of the village of Moron de la Frontera and Gilena (both near Seville, Spain) (see Table 2). The Limestones belong to geological the Unit of the *Sierra de Estepa* (External Zones Betic Chain, Spain) of age lower and mid-Jurassic [44].

In order to know how the calcination temperature affects the physical properties of CaO, these two varieties of limestones have been calcined in a muffle at different temperatures (800–1000-1100 °C) and 1 atm of partial pressure of CO_2, in grain sizes of several centimeters and with a residence time in the muffle of 60 min.

2.3. Methods

The mineralogical composition of the materials was evaluated by X-ray diffraction (XRD), using a Philips PW-1710 diffractometer

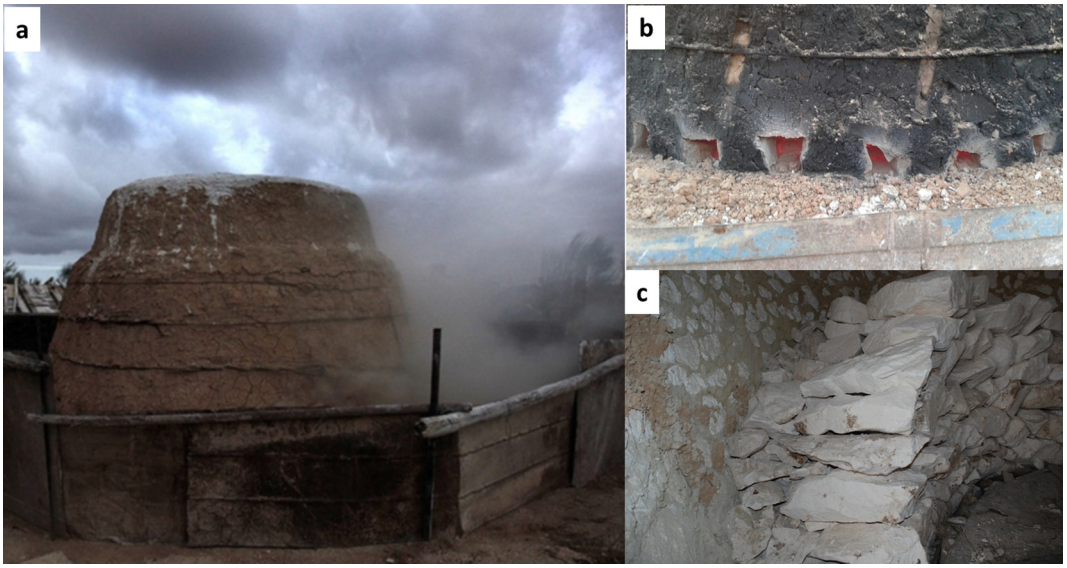

Fig. 1. a) Traditional lime Kiln. b) Caños o troneras c) *Ahornado* process, method of dry stone, built with *armaderas* (larger stones) in a concentric arrangement.

Table 1
Quicklime samples analyzed.

Quicklime samples	Temperatures (°C)
CaO(TL). Traditional method. Gordillós lime	1100 900
CaO(IL). Industrial method. Calcinor, Andalusian of Limes	Around 1000
CaO(PL). Analytical purity. PANREAC AppliChem.	

Table 2
Limestone samples from *Unit of the Sierra de Estepa* (External Zones of the Betic Chain, Spain).

Quarries samples	Location
M-1	Historic quarry from Morón de la Frontera, Seville. Spain
G-1	Gilena quarry, Seville, Spain

with an automatic slit. Measurement parameters were as follows: Cu Kα radiation (λ = 1.5405 Å), an exploration range from 10° to 80° 2θ, steps of 0.023° 2θ s^{-1}. The chemical composition of major elements and Loss on Ignition (LOI) was done using the Phillips X-ray Fluorescence (XRF) minitraces method and PANalytical AXIOS Rh spectrometer. Analysis of the shape, size, and ultrastructure of quicklime samples was performed by means of scanning electron microscope (SEM), FEI Jeol 5400X, field emission scanning electron microscopy FESEM (FEI-TENEO), acceleration voltage: 200 eV–30 KeV (20 eV with BD) and HRTEM by using a Philips CM20, operated at a 200 kV acceleration voltage. Prior to HRTEM observations the samples were gently ground in an agate mortar and dispersed in ethanol, sonicated 60 s, and deposited on Formbar-coated copper grids. HRTEM observations were performed using a 40 μm objective aperture. SAED patterns were collected using a 10 μm aperture, which allowed collection of diffraction data from a circular area of 0.5 μm in diameter.

The N_2 sorption isotherms were obtained at 77 K on a Micromeritics Tristar 3000 under continuous adsorption conditions. Prior to measurement, powder samples were heated at 200 °C for 2 h and outgassed to 10^{-3} Torr using a Micromeritics Flowprep. BET analysis was used to determine the total specific surface area (SSA). The total pore volume (V_{Total}) and micropore volume (V_{micro}) of the samples were calculated using t-plot analysis. The BJH method was used to obtain pore size distribution (PSD) curves.

Thin sections of quarry stones were examined with a Leica DMLP petrographic polarizing microscope and a camera with a Leica DFC 280 digital image capture system.

The reactivity test of quicklime was carried out according to ASTM C110 standard Test [45]. This analysis allows to indirectly measuring the slaking process time of lime during the hydration of quicklime. The method consists of preparing a sample of quicklime that passes the N° 6 ASTM sieve (3.35 mm), 50 g is introduced into 100 ml of distilled water with stirring. The temperatures measurements of the system are taken until a change of less than 0.5 °C is verified in three consecutive readings. At the same time, data on the variations in pH and electrical conductivity have been taken.

3. Results

3.1. Mineralogical-petrographic, chemical and microtextural analysis of limestones and quicklimes

3.1.1. Limestone

Mineralogical composition data of the limestones used for lime production, M-1 and G-1 lithotypes was very similar, with average calcite contents of 100%. Chemical composition data of major elements of the two lithotypes can see in Table 3. The data also indicate similar chemical compositions, both correspond to very pure limestones with less than 1% in impurities.

The petrographic observations indicate that the M-1 lithotype corresponds to an oosparite limestone [46,47], with a predominance of micritic intraclasts of ooids, abundant crinoids plates and sparite and micritic cement (see Fig. 2a). This limestone also presents important contents in intergranular and intragranular macropores, semi-filled of calcareous sparite cement (>200 μm). The G-1 lithotype corresponds to an oomicritic limestone [46,47] constituted by micritic ooids and crinoids plates with little intergranular cement and abundant intergranular macroporosity (around 100 μm), also filled of calcareous sparite cement but in a smaller proportion (see Fig. 2b).

The microtextural observations show that the M-1 and G-1 lithotypes corresponds to limestones of similar compositional but with differences macropores volume and crystallinity. FESEM observations prove that the M-1 lithotype presents of large crystals of size around 400 μm (crinoid plates), sparite cement of size around 30 μm and the presence of macropores of maximum size around 50 μm (see Fig. 3a). In the G-1 lithotype (see Fig. 2b) predominance of micritic cement (around 2 μm) although pores filled with calcareous sparite cement (around 15 μm) and intercrystalline macroporosity (20 μm) are observed.

3.1.2. Quicklimes

Mineralogical composition data of the different quicklimes indicated in the Table 4. The CaO(TL) has a lower lime (CaO) content and a higher content of portlandite ($Ca(OH)_2$) than the CaO(IL) or CaO(PL). This may be related to the process of lime handling. In this table the density data are also indicated, the results shows that the CaO obtained in the traditional lime kiln have lower density.

Chemical composition data of major elements (see Table 3) indicate that quicklimes are very pures (>88% CaO). It notes for the quicklimes (IL and PL) a greater content in impurities (SiO_2, Al_2O_3 and Fe_2O_3). On the other hand the CaO(PL) shows the lower LOI values, indicating a calcinations complete or minimal recarbonation (see Fig. 4). The CaO(TL), present the highest LOI, indicating presence of carbonates, these values are higher in the CaO(TL1). This can be explained because in these kilns the calcination is carried out on large fragments, and the existence of uncalcined areas is more likely. However, some authors have shown that reach to the degree of dissociation of carbonates up to 100% is not recommended because it decreases kiln productivity and increases the specific fuel consumption for calcination. In practice it is limited the degree of dissociation of the material at 90–98%. [49].

SEM microtextural observations of the CaO(TL1) let you see the development of a very thin sintering discontinuous surface layer and under this layer the presence of CaO crystals of variable size, from 5 to 20 μm (see Fig. 5a, b), associated with areas where the temperature can reach 1100 °C. The CaO(TL2) shows a smaller grain size (around 5 μm) but more homogeneous, in areas where the temperature reached 900 °C (see Fig. 5c). It is note in the Fig. 5d how the crystals of CaO have grown on the surface of original calcite crystals presenting more rounded shapes and porous and rough surfaces. They have a smaller grain size (around 3 μm) and are related to areas where the temperature does not exceed 800 °C. This confirms the incidence of the calcination temperature on the size of the CaO crystals [14,18]. These observations show that in areas where the CO_2 pressure and temperatures are higher, crystals of more heterogeneous size are formed (areas closer to the heat source) and in the areas of the kiln where the pressure is closer to equilibrium, the size of the CaO crystals is makes more homogeneous and smaller when temperatures are lower (in the areas farthest from the heat source.).

Table 3
Chemical composition data of major elements, expressed in wt% of oxides, of limestone and quicklime samples. Loss on Ignition (LOI).

Samples	SiO_2	Al_2O_3	Fe_2O_3	MnO	MgO	CaO	Na_2O	K_2O	TiO_2	P_2O_5	LOI
M-1	0.11	0.03	0.02	0.01	0.2	55.02	0.03	0.02	0.01	0.01	43.51
G-1	0.03	0.01	0.01	0.01	0.12	54.52	0.02	0.01	0.01	0.08	44.16
CaO(TL1)	0.18	0	0.06	0	0.38	88.1	0.03	0.02	0	0.05	11
CaO(TL2)	0.15	0	0.04	0.02	0.35	88.7	0.03	0.02	0	0.08	10.6
CaO(IL)	0.37	0.1	0.09	0.02	0.52	93.4	0.03	0.05	0	0.05	5.22
CaO(PL)	0.1	0.27	0.28	0.02	0.6	95.86	0.02	0.02	0	0.02	1.6

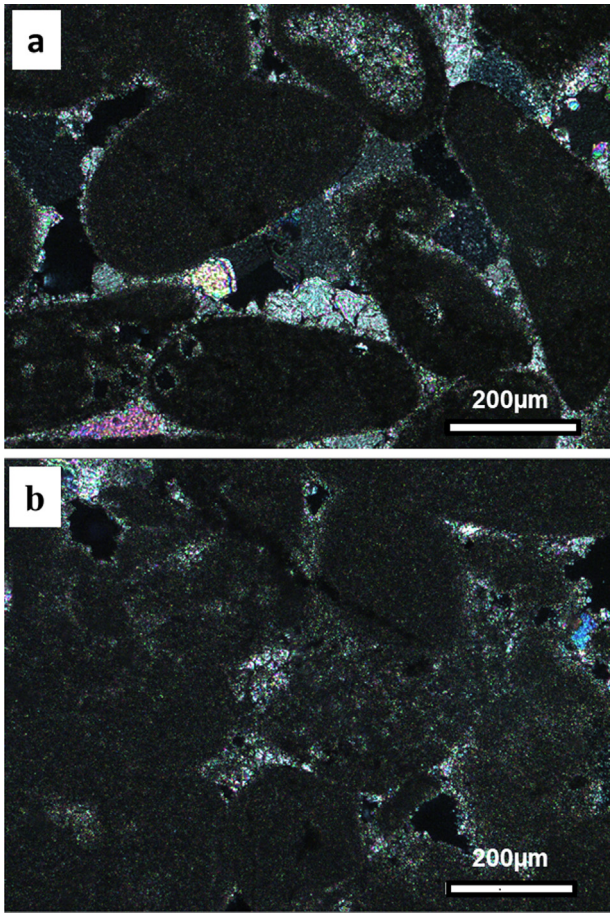

Fig. 2. Petrographic observations of limestones used in the production of quicklimes (plain polars). a) M-1 lithotype, oosparite limestone. b) G-1 lithotype, oomicritic limestone.

FESEM microtextural observations of the CaO(TL2) allows to see the presence of CaO crystals very porous (intergranular porosity range from 3 to 5 μm) with rough surfaces that have not experienced sintering (see Fig. 6a, b). The development of rough surfaces and microporous can indicates calcination process with a higher concentration of water vapor, less sintering and temperature and more progressive decarbonation rate [5].

On the other hand FESEM microtextural observations has also allowed to see the heterogeneity of the calcination process of the limestones in an industrial kiln CaO(IT). In Fig. 7a; an area is observed where the heat has produced microcracks in the stone, which indicates rapid heating without significantly affecting the microtexture of the limestone. In other areas the formation of pockets of oriented CaO crystals with straight edges parallel to the planes of calcite are observed (see Fig. 7b), which indicates that the heating has caused small modifications in the microstructure of the limestone. The size of the original, little transformed crystals, indicate that the type of limestone used is the M-1 lithotype. Areas with sintered surfaces have also been observed on calcite crystals with rounded appearance; smooth surfaces, crack porosity and intercrystalline porosity closure (see Fig. 7c). In other areas the microtextural of these sintered surfaces become more porous (see Fig. 7d), where the CO_2 output is most likely. This cause increased internal pressure within of material that finally explodes producing CaO smaller crystals of around 1 μm and an intergranular porosity around 1 μm (see Fig. 7e). These structures can be explained because if the temperature rise is too rapid, the surface layers of the limestone are calcined very fast, consequently shrinkage of volume and intercrystalline porosity reduction is produced. Due internal pressure within the limestone finally explodes producing smaller crystals as result of mechanical stress accumulated among crystals.

FESEM microtextural observations of CaO(PL) allows to see CaO crystals with spherical shapes of size between 1 and 2 μm (see Fig. 8a, b) and symphysis of these crystallites, but with a greater micro-textural homogeneity (crystals size and porosity). These microtextures could be explained because in conditions of lower Pco_2 (next to equilibrium pressure), the size of the crystals is reduced by the increase of the temperature. On the other hand, the dominant mechanism at low partial pressures of CO_2 for the growth of the CaO crystal would be the sintering of the nanocrystals by reticular diffusion, which is favored by the increase of the temperature [26]. This indicates that the calcination conditions of

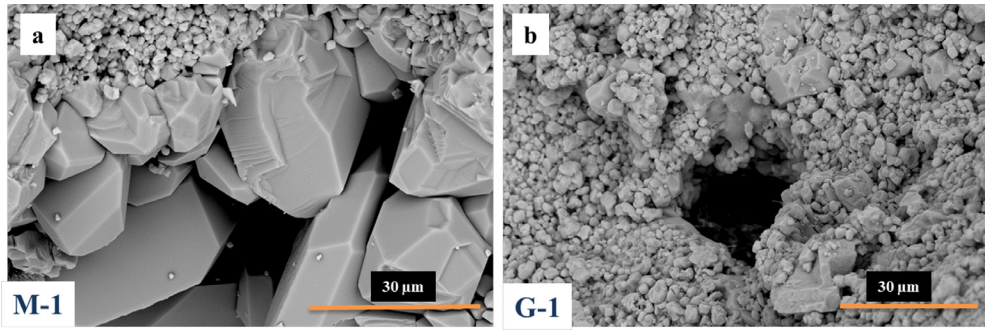

Fig. 3. FESEM microtextural observations of the limestones used to obtain the quicklimes a) M-1 lithotype. Cement of secondary origin (size >30 μm) are observed. b) G-1 lithotype. Predominance of micrite calcite crystals (around 2 μm) and intercrystalline macroporosity (around 15 μm) are observed.

Table 4
Mineralogical composition data of quicklime samples, expressed in wt% and density (g cm^{-3}).

Samples	Lime %	Portlandite %	Calcite %	Density (g cm^{-3})
CaO(TL1)	81.8	12.5	0	3.199
CaO(TL2)	90.4	5.1	0	3.287
CaO(IL)	93	2	0	3.346
CaO(PL)	100	0	0	3.346

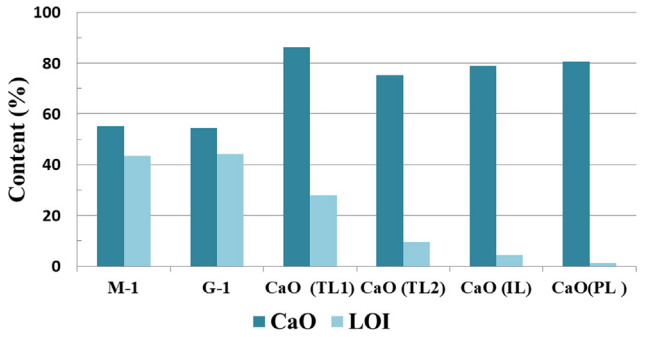

Fig. 4. Content in CaO and Loss on Ignition (LOI) of the limestones and quicklimes calcined in the laboratory.

the limestone have been rapid heating but in conditions of CO_2 pressure next to equilibrium, which has allowed the total calcination of the stone favored by the escape of CO_2 continuously.

HRTEM and electrons diffraction pattern (SAED) images of the different CaO can see in Fig. 9. Debye rings provides information on the microstructure of the CaO, orientation and size crystals. These CaO presents different Debye rings: diffuse, spotty, nearly continuous; according to the different production technologies. Note that a preferred orientation of CaO crystals is detectable by the brighter spots in the Debye rings for the CaO(TL1). These patterns SAED define thick rings indicating larger crystals associated with randomly oriented of CaO nanocrystal (Fig. 9a). In the CaO (TL2) observe more continuous and homogenous Debye rings indicating less crystallographic orientation of the CaO crystals and smaller and homogeneous size (see Fig. 9b). On the contrary HRTEM observations of the CaO(IL) and CaO(PL) indicate a greatest oriented of grains, since the Debye rings are not observed, indicating also a more sintering structure (see Fig. 9c, d). Crystals attach along equally oriented faces during aggregation, thus minimizing surface energy [18]. However in the CaO(IL) X-ray diffraction patterns of partially converted CaO show the presence of diffraction spots from the parent calcite crystal and a diffuse rings of the CaO crystals, indicating remains of calcite inside of the particle.

These microtextural observations carried out on the different CaO indicate that in the traditional lime kilns less oriented and sintered structures and larger crystals are formed. It is verified that the increase of the temperature in this type of kilns favors the aggregation and orientation of crystals of CaO. On the other hand the rapid heating, that usually takes place in industrial lime kilns, favors the development of oriented structures of CaO crystals and the high pressures of CO_2 inside the particle hinder the development of the calcination process of the limestone. The high temperature favors the rapid formation of CaO with smaller crystals.

3.2. Physical characterization of stone and quicklime calcined in the laboratory

3.2.1. Limestones

The quarries stones analyzed (M-1 and G-1) correspond to very compact limestones, their physical properties have been previously studied by [48]. These authors establish two groups (I group and II group) within the Unit of Sierra de Estepa (External Zones of the Betic Chain, Spain), based on their physical properties (density, porometry and surface area). Correspond to a few porous limestones (2–13%) and values in surface area from 0.36 to 0.96 $m^2.g^{-1}$, in the two groups of limestones (see Table 5).

The I Group presents lower density and surface area that the II group, with predominance of macropores of size from 0.1 to 0.2 μm. The II group presents higher spectrum of porosity and

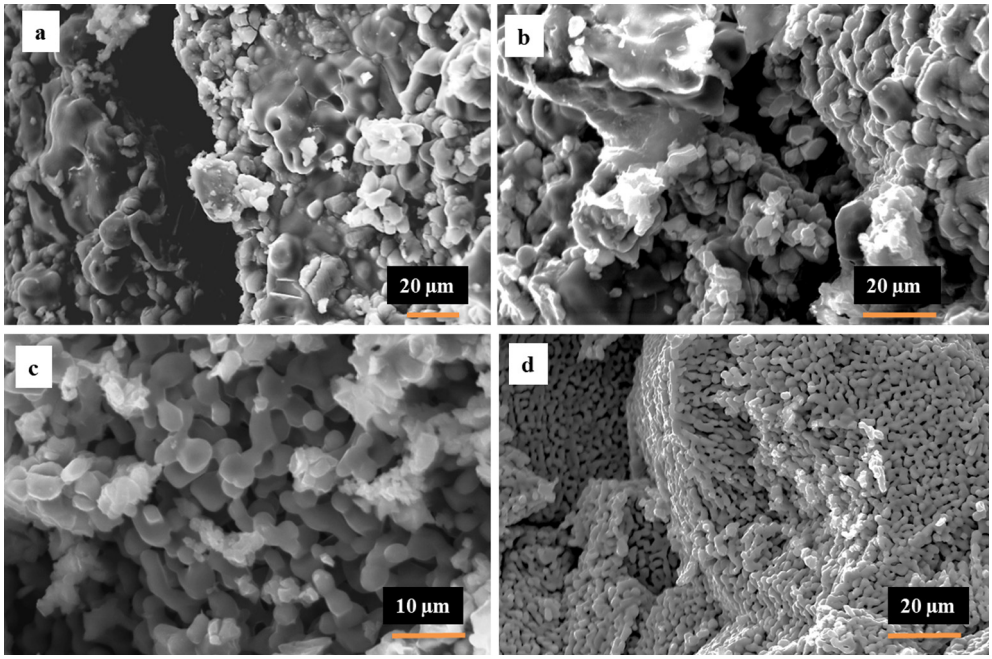

Fig. 5. SEM microtextural observations of CaO(TL1) and CaO(TL2). a-b) CaO(TL1). A very thin sintered layer and particle size ranging from 10 to 20 μm are observed. c) CaO (TL2). It can see crystals of CaO formed at 900 °C, with grain size of around 5 μm and intercrystalline porosity. d) CaO(TL). Formation of nanocrystals of CaO on the surface of the faces of the original calcite crystals and corresponds to areas where the temperature does not reach 800 °C, presenting a smaller grain size.

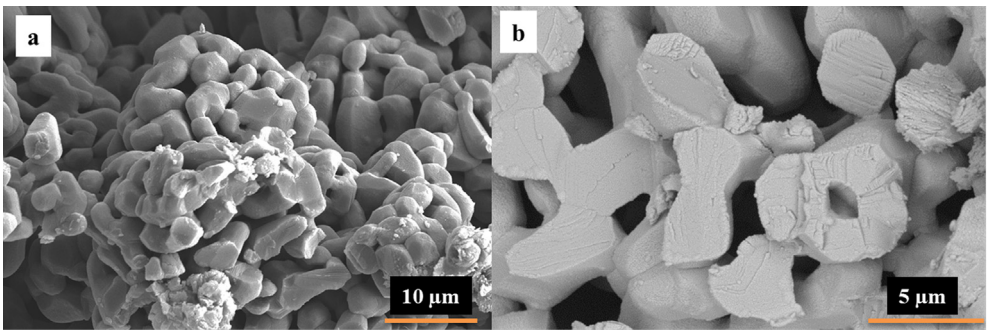

Fig. 6. FESEM microtextural observations of CaO(TL2). a) Intergranular porosity from 3 to 5 μm is observed. b) CaO nanostructure formed by oriented attachment mechanism is observed.

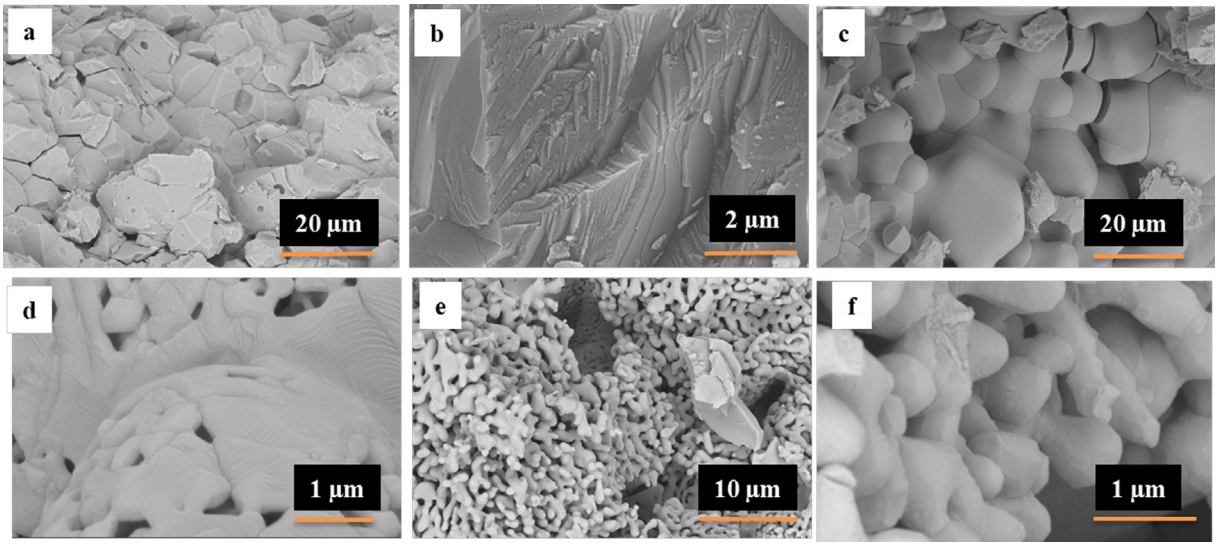

Fig. 7. FESEM microtextural observations of different stage of the calcination process of CaO observed in the quicklime from industrial kiln, CaO(IL). a) First stage, rounding of the faces of the original calcite crystals and the presence of cracks by shrinkage. b) Formation of pockets of oriented CaO crystals is observed with straight edges parallel to the edges of calcite. c) Rounding of the faces of the CaO particles d) Second stage, development of microporosity output of CO_2 due to the effect of heating. e, f) Final stage, development of very porous structures indicating the complete transformation of calcite to CaO with sub-rounded shapes and smooth surfaces.

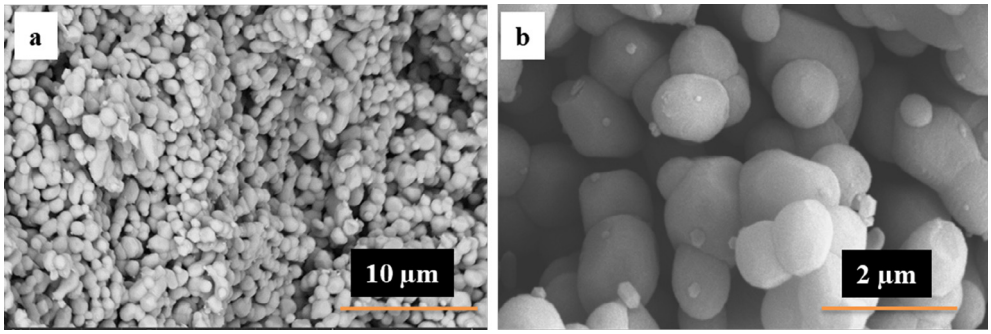

Fig. 8. FESEM microtextural observations of CaO(PL). a) Development of very porous structures between CaO crystals. b) Development of rounded shapes of the crystals and size about 1 μm in the CaO(PL) with rounded shapes and smooth surfaces.

bimodad tendency; a first range around at 0.02 μm and a second range from 0.3 to 1 μm. Its highlight that the two lithotypes of limestones studied in this paper is correlated with these two limestone groups established by [48].

3.2.2. Quicklimes obtained in laboratory

Physical properties data of quicklimes obtained in the laboratory at different temperatures are shown in the Table 6. The calcination process produces changes in the surface area and total pores volume in the two types of limestones (see Fig. 10). Increases the surface area and pore volume are produced and these values are higher at 1000 °C in the two types of limestone, coincident with the works by [49].

At 800 °C the surface area of the M-1 lithotype is 0.7 $m^2.g^{-1}$ (within the margin set for the limestones of group I) and in the G-1 lithotype is 5.849 $m^2.g^{-1}$ (values well above the margin set

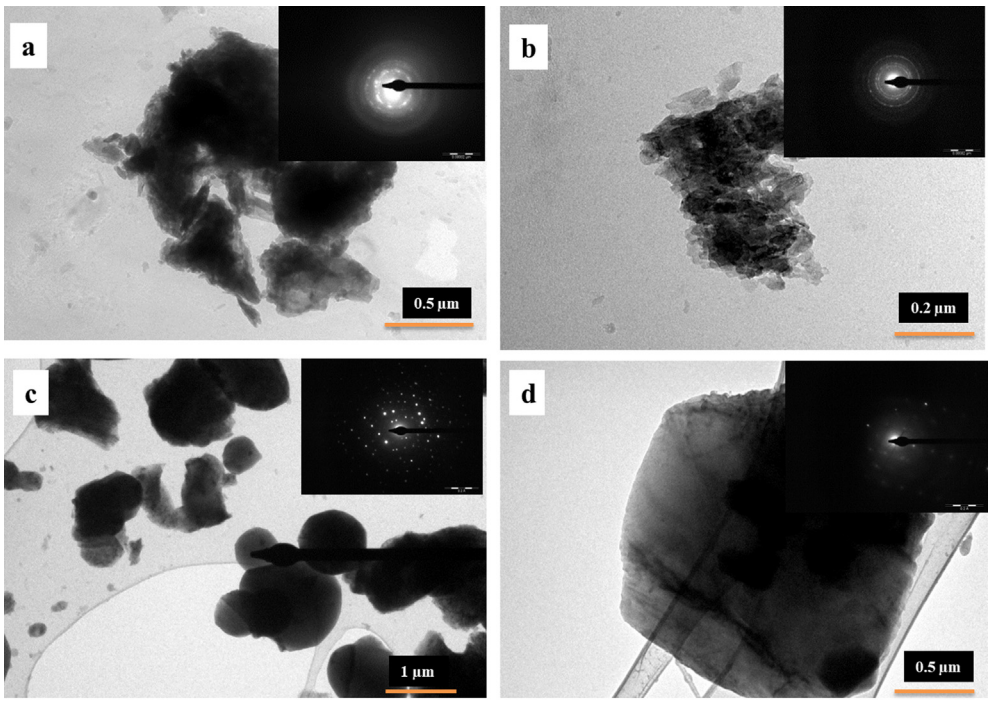

Fig. 9. HRTEM images (SAED in inset) a) Clusters formed by apparently oriented CaO(TL1) crystals. Transformation into an aggregate of CaO crystals showing a SAED pattern with spotty, nearly continuous and thick Debye rings b) A diffuse and discontinuous Debye rings but the distance between Debye rings is smaller, which indicates smaller size of crystals. c, d) In CaO(IL) and CaO(PL) the Debye rings are not observed indicating a more sintering structure.

for limestone), at the same temperature and similar residence time in the muffle. This indicates that the textural characteristics of the rock (crystallinity and porosity) affect its behavior during heating. When the temperature exceeds the optimum heating limits, the microstructure of quicklime becomes less porous. This explains the significant reduction of the microporosity at 1000 °C in the G-1 lithotype; while the M-1 lithotype continues to increase its porosity [13,50]. The rocks with smaller crystal sizes had greater surface area and therefore burning would be more rapid [39] and the sintering can take place at a lower temperature.

The Table 6 also shows the evolution of pore size, surface area and volume of micropores due to heating, in the two limestones. The data indicates that the temperature increase generates greater volume of micropores, up to 1000 °C in the lithotype M-1 and up to 800 °C in the lithotype G-1. Exceeding these temperature limits the quicklimes lose their microporosity or is significantly reduced, as is the case of the lithotype M-1. This indicates that the more crystalline rocks have greater resistance to heating. These aspects also affect the pore size of these quicklimes. The G-1 lithotype increases the pore size with temperature unlike the lithotype M-1, which is significantly reduced. The sintering process, according to the data, implies a decrease in the volume of micropores but an increase in pore size that may be related to the formation of cracks due to thermal stress and shrinkage [8,19].

N_2 adsorption isotherms data of quicklimes at different temperatures is shown in Fig. 11a, b. The M-1 lithotype at 800 °C presents predominance of mesopores (according to IUPAC) of size around 0.02 µm (200 Å), similar to the pore size distribution observed in the limestones of I Group defined by [48], and increase pore of size around 0.05 µm (500 Å). When the temperature reaches 1000 °C there is an increase of porosity in the range from 0.01 to 0.04 µm (tendency similar to the G-1 lithotype at 800 °C). In the G-1 lithotype, when reaches 1000 °C, there is a reduction of mesopores, although the spectrum remains similar to M-1 lithotype (range from 0.015 to 0.03 µm and to 0.05 µm). At 1100 °C the two rock lithotypes shows a drastic reduction in porosity and homogenization in the pore size distribution (within the same range) greater in the G-1 lithotype.

The data indicates that during the calcination process in the range from 800 to 1000 °C there are important variations in the micro-textural evolution depending on the type of limestone, but exceeded this temperature range the pore size is significantly homogenized, with a reduction in grain size in the spectrum between 100 and 500 Å. In the first phases of calcination (at 1000 °C for the M-1 lithotype and at 800 °C for the G-1 lithotype) two groups of pores are generated, which can be related to the development of micro-cracks due to thermal stress, pores that disappear at high temperatures.

The surface area and total pores volume increases with temperature in quicklime obtained in laboratory, with a reduction of the microporosity and increase of the maximum pore size. When the temperature reaches very high values, the total pores volume and microporosity and macropores are reduce; where the micro-textural characteristics of the limestone have an important impact. The specific surface area evolution can be explained by combining the effects of the grain growth and the pore size distribution [51]. The less crystalline limestones the reduction in porosity is greater, indicating less resistance to thermal stress.

Table 5
Physical properties data of the quarries limestone by [39].

Samples	P_T (%)	Density (g. cm^{-3})	Surface area ($m^2.g^{-1}$)
I Group. oncolitic limestones coarse grain	2.42–13.25	2.66–2.85	0.44–0.96
II Group. oncolitic limestones fine grain	2.7–10.32	2.67–2.82	0.036–0.87

3.2.3. Quicklime calcined in lime kilns

Physical properties data of the CaO obtained in the different lime kilns are shown in Table 7, including the sample of analytical

Table 6
Physical properties data of limestones and quicklimes calcined in the laboratory.

Samples	Surface area ($m^2\ g^{-1}$)	Total pore volume ($cm^3\ g^{-1}$) (17–3000).10^3Å	Micropore volume ($cm^3\ g^{-1}$ STP)	Pore size (Å)
M-1 T1(800 °C)	0.7019	0.001613	–	137.794
M-1 T2(1000 °C)	5.7073	0.017053	0.000371	135.224
M-1 T3(1100 °C)	2.6188	0.005964	0.000330	123.598
G-1 T1(800 °C)	5.8492	0.018502	0.000184	137.794
G-1 T2(1000 °C)	8.1429	0.029089	–	147.311
G-1 T3(1100 °C)	0.7019	0.001613	–	151.162

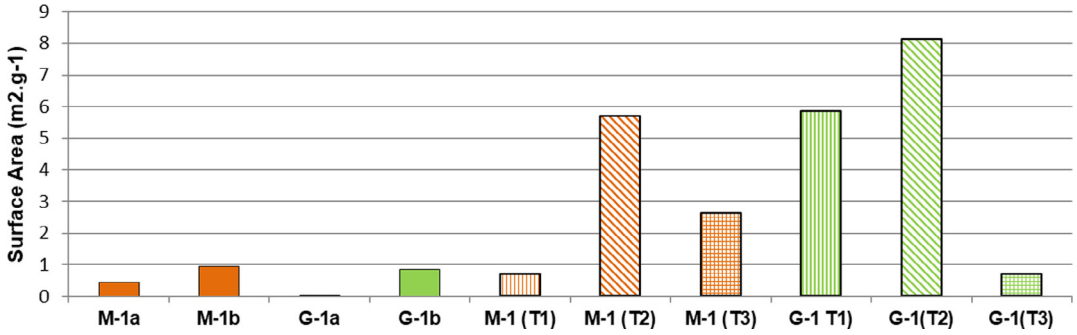

Fig. 10. Surface areas of limestone and quicklime calcined in the laboratory.

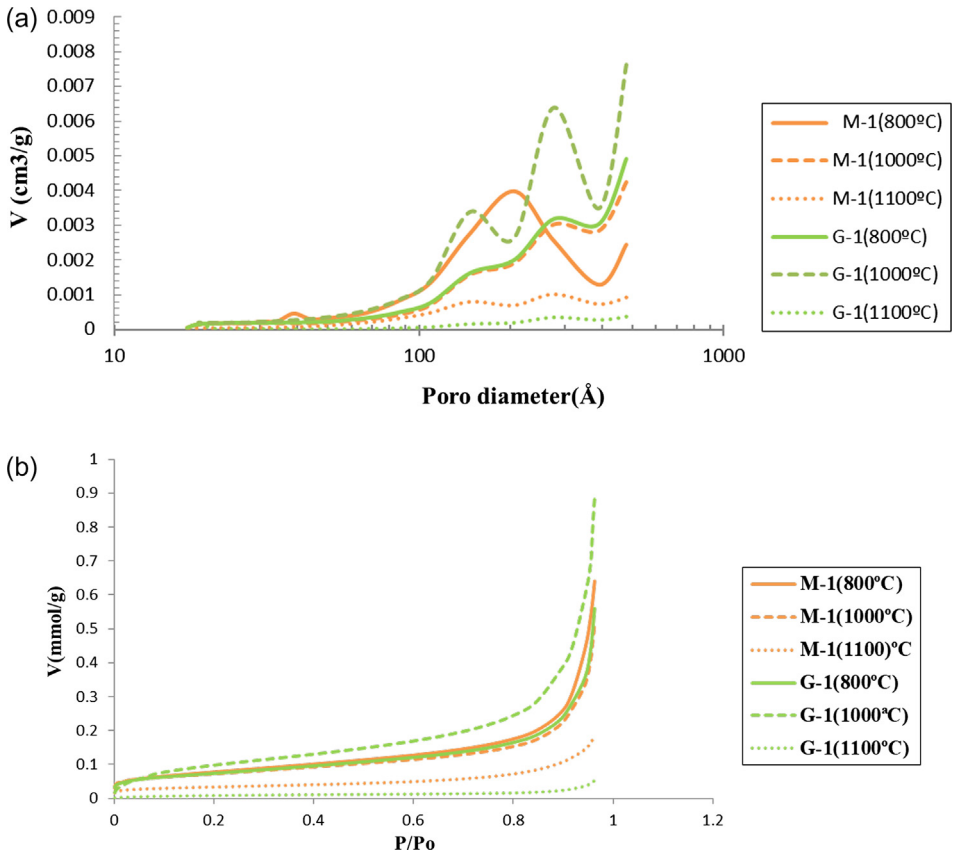

Fig. 11. a) Pores size distribution of quicklimes calcined in the laboratory (PSD) b) N_2 adsorption isotherms of M-1 and G-1 samples calcined in the laboratory at 800–1000–1100 °C.

purity CaO(PL). The surface area, total pores volume and predominant pore size data of the quicklimes obtained in the laboratory are greater than those observed in the lime kilns (traditional and industrial) (see Fig. 12). This could be related to temperatures reached, P_{CO2} and/or residence time in the kilns.

N_2 adsorption isotherms data of quicklimes from the different kilns are indicated in the Fig. 13a, b. The similar values of pore size distribution (20–500 Å) are highlighted, with variations in a very narrow range of porosity. The variations are in the range established by the two lithotypes of rocks (M-1 and G-1) calcined at 1100 °C; including CaO(PL), obtained from another type of rock. This is indicating of the importance of the calcination temperature in the physical properties of quicklimes and on the other hand that the temperatures reached in this kilns define the same distribution of pore size for all quicklimes, with variations in the micropores and mesopores volume.

The CaO(TL1) and CaO(PL) present higher total pore volume and the range of micropores is absent, this may indicate higher calcination temperatures for these quicklimes. On the other hand surface area and total pores volume data of the CaO(TL1) indicate values similar to the quicklime from M-1 lithotype (at 1100 °C) (see Table 6), coinciding with the temperature set for CaO(TL1). This corroborates the incidence of the microtextural and chemical characteristics of the limestone in the physical properties of the quicklimes.

The CaO(TL2) and CaO(IL), originated at a similar temperature (around 900 °C) but different production technology, have lower values of surface area, total pores volume and greater microporosity that CaO(TL1) and CaO(PL). However there are differences of interest between these two types of quicklimes; the CaO(TL2) presents less surface area, larger pore size, greater total pore volume and lower microporosity. This indicates that quicklimes obtained in industrial lime kilns generate CaO nano with less content in mesopores and with more surface area due to the higher content in micropores and predominantly smaller pore size. However, the temperature has an important impact on its microstructure based on data obtained for these last two CaO. In this work, we have been able to verify that in the traditional lime kilns the CaO have a larger predominant pore and crystal size and this is not only related to the calcination temperature and crystalline and compositional characteristics of the original limestone. The production technology of lime in a traditional kiln must have a significant impact. Previous works indicate that increase of the calcination temperature and time make that the pore size distributions of nano CaO were not uniform, on the other hand increasing the calcination temperature make that the CaO grain size to increase and the growth rate to accelerate, although the growth was not unlimited [51].

The calcination process in these traditional lime kilns occurs under conditions more controlled of pressure of CO_2 and temperatures; because the fuel used is wood [8] and the calcination process need longer residence time in the kiln. These conditions can increase the porosity, with greater development of microcracking favored by the higher concentration of steam [9]. The pores formed in these conditions are in the range from meso to macropores (between 0.05 and 1 μm) [15]. The calcination with steam can occur at a lower temperature, but it needs longer residence time [21]. In these conditions can generate more porous nanotextures with a larger pore size. These conditions can occur in this type of kilns since the calcination takes place on fragments of larger limestones and the transmission of heat through the material is more progressive.

In the industrial lime kiln, the quicklimes generated are characterized by greater microporosity, this may indicate agglomeration of small crystals and closure of pores related to sintering. However, the growth of grain size should also have a significant incidence [51], which would explain the characteristics of CaO(PL) with an important volume of mesopores, high surface area and smaller predominant pore size related to a lower grain growth rate.

3.3. Reactivity of quicklime

Previous works indicate that the quicklime slaking process depends of the conditions of calcination of the limestone; the temperature, surface area and size of the CaO particles are the factors that most affect [9,52]. The rate at which quicklime is hydrated increases with increasing lime surface area and the slaking temperature, and the higher the calcination temperature is less active quicklime [52]. The kinetics of the reaction is given in a first phase by the reaction (2), subsequently occurs the dissolution of $Ca(OH)_2$ to give Ca^{+2} and OH^- ions in solution and finally the diffusion of these ions in the solution, where the size of the grains has a significant effect [53].

Reactivity test data according to ASTM Standard [45] realized on the different quicklimes is shown in the Table 8, includes slaking temperature, pH and electrical conductivity. The data indicate significant variations in terms of slaking time, maximum temperature reached, pH evolution and electrical conductivity between the different quicklimes.

The kinetic behavior of the reaction according to the temperature vs time profiles, for different quicklimes, defines two phases: first phase corresponds to the solid-liquid interfacial reaction, between quicklime and water, and the second to the gas-solid reaction, between water vapor and CaO. This last chemical reaction can be affected by extremely rapid heat release and thermal and mechanical stresses inside the solid body [54]. The CaO(IL) plot shows a first phase of rapid reaction of quicklime with the water and a large heat release (see Fig. 14a). The CaO(PL) plot also defines a first phase of rapid reaction, although without a significant heat increase. The quicklime produced in a traditional lime kilns are characterized by a slower first reaction phase; although differences are observed between the CaO(TL2) and CaO(TL1), in the latter case the reaction implies less heat release and greater slaking time. This means that quick lime calcined at higher temperature becomes less reactive coincident by [55].

The data indicate that the porosity of CaO affects the slaking temperature, the higher the mesoporosity the lower the slaking temperature, and the size of the particles affects the slaking time, the larger the particle size, the longer the slaking time.

The evolution of pH versus time for different quicklimes is shown in the Fig. 14b. In the slaking process the diffusion

Table 7
Physical properties of the quicklime samples from different lime kilns.

Samples	Surface area ($m^2\ g^{-1}$)	Total pore volume ($cm^3\ g^{-1}$) (17–3000).10^3Å	Micropore volume ($cm^3\ g^{-1}$ STP)	Pore size (Å)
CaO(TL1)	2.2659	0.004937	–	98.954
CaO(TL2)	1.1278	0.002879	0.000100	130.139
CaO(IL)	1.6988	0.001961	0.000293	85.271
CaO(PL)	2.3210	0.004202	–	82.658

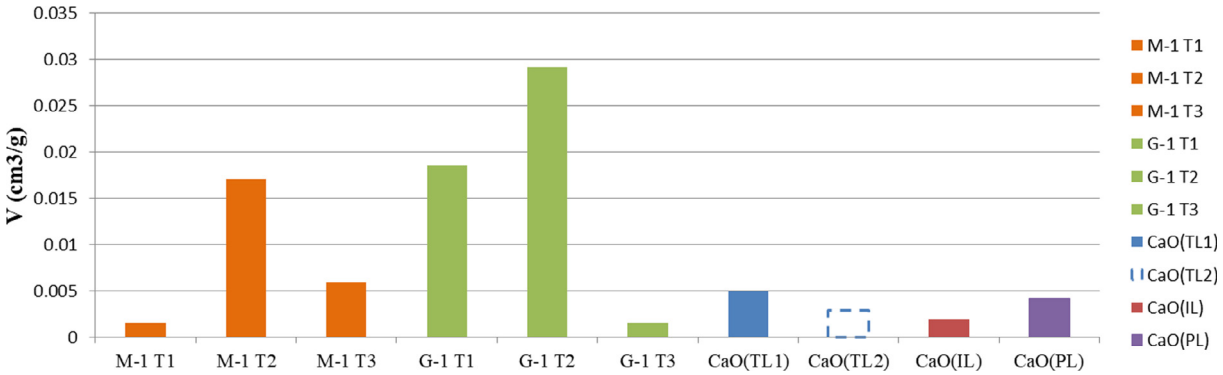

Fig. 12. Total pore volume of limestone and quicklimes calcined in the laboratory and kilns.

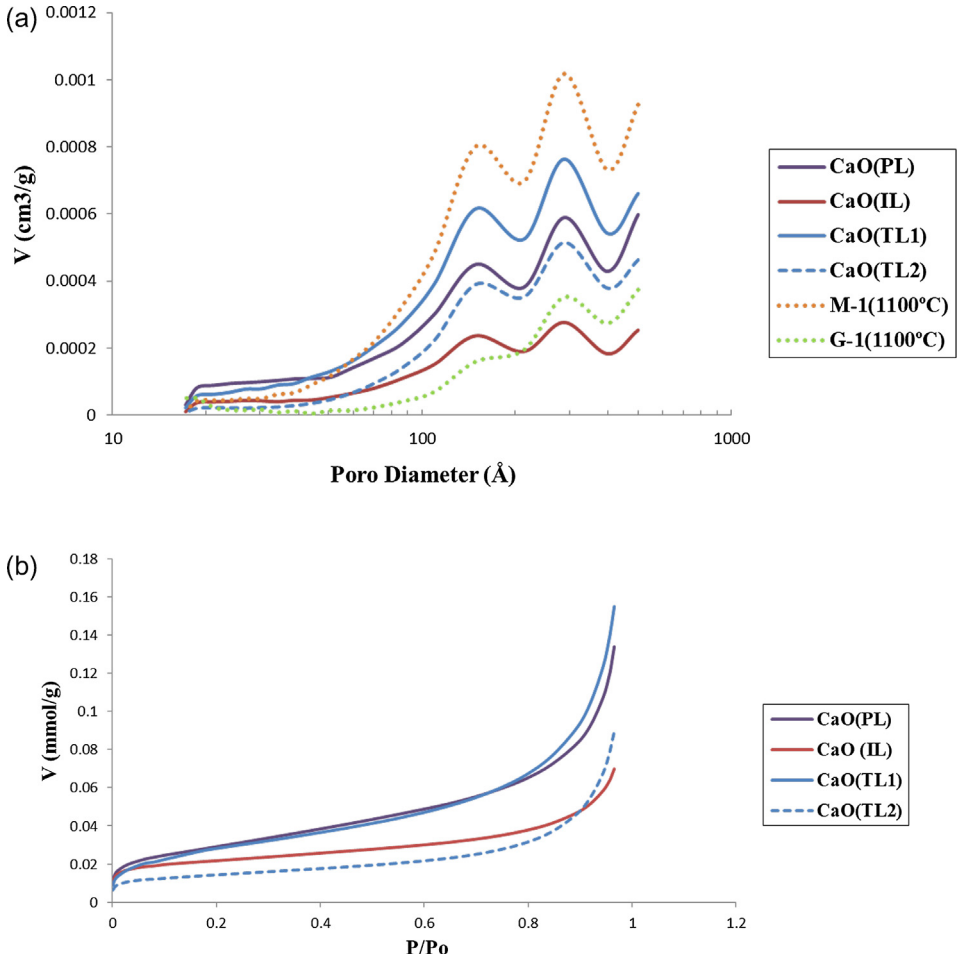

Fig. 13. a) Particle size distribution of CaO(TL1), CaO(TL2), CaO(IL) and CaO(PL). b) N_2 adsorption isotherms of CaO(TL1), CaO(TL2), CaO(IL) and CaO(PL).

Table 8
Temperature, pH and electrical conductivity data of quicklimes (reactivity test) with respect to time (minutes).

CaO Type	T_{max} (°C)	Time (T_{max}) (m)	pH	Time (pH_{max}) (m)	Conductivity (μS/cm)	Time (C_{max}) (m)
CaO(TL1)	32.9	40.5	12.55	12.5	10.63 (1.5 m)	1.5
CaO(TL2)	59.6	15	12.58	1	5.87	0
CaO(IL)	76.6	3.5 m	12.52	0	9.034	0
CaO(PL)	45.4	5.25	12.11	0	3.68	0

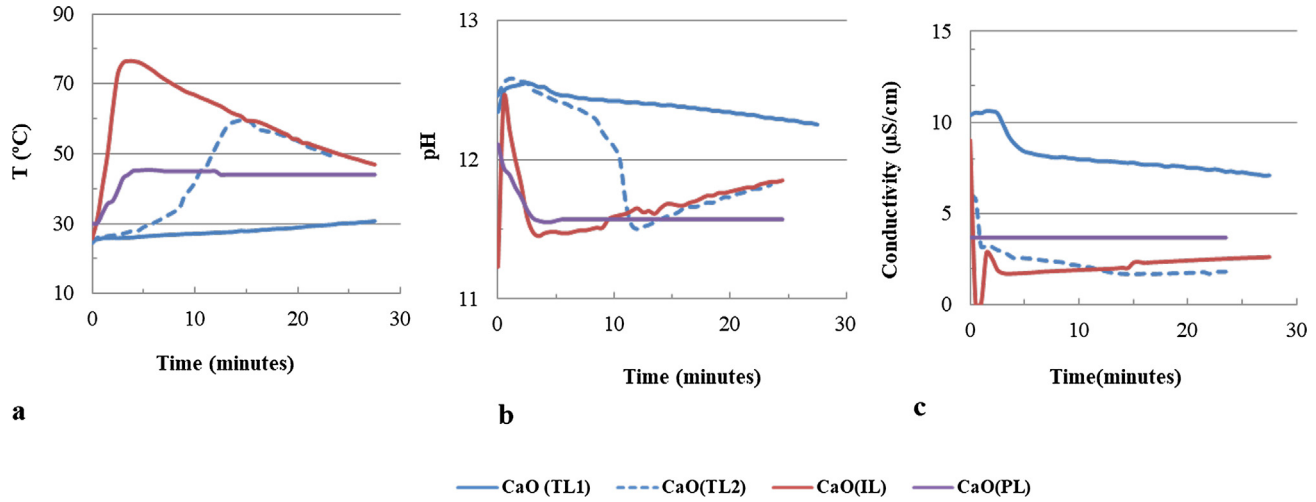

Fig. 14. Reactivity tests data. a) Temperature versus time. b) pH versus time. c) Electric conductivity versus time.

coefficient of $Ca(OH)_2$ depends quite strongly on the ions concentration. The high concentration of Ca^{+2} and OH^- ions are responsible of the reaction rate, where the OH^- ions seem to have more incidences [52,53]; therefore the formation of calcium hydroxide involves a decrease in the pH of the solution.

The CaO(IL) and CaO(PL) plot shows a rapid increase in pH (>12) in the first moments of the reaction and rapid decrease of pH values (11.5). On the other hand, the CaO(TL1) and CaO(TL2) plot defines high pH values that keep high for longer, where CaO(TL1) maintains constant values during the control time. Therefore a greater concentration of OH^- ions in the slaking solution implies to reduce the slaking rate.

The opposite trend of the curves temperature vs time and pH vs time, indicate that the slaking rate decreases with the pH and increase with the temperature. These results coincide with the previously mentioned works and by examining these graphics it is possible to demonstrate to what degree the solubility of the CaO are related to their microtextural changes.

The ionic or electrical conductivity of an aqueous solution is due to the movement of the ions in solution and will depend, equal voltage and charge, of the mobility of the present ions. The evolution of electrical conductivity vs time for different quicklimes is shown in the Fig. 14c. The reaction defines a first phase with high conductivity and second phase with decrease, in all the quicklime types. In the CaO(IL) plot two peaks of rapid descent at the beginning and progressive recovery until equilibrium are described. The CaO(TL2) plot present a rapid decrease in the initial phase and progressive decrease towards values similar to CaO(IL). The CaO(PL) plot the values remains constant similar to CaO(TL1), but the latter with higher values of electrical conductivity. This is indicating to us that the quicklime produced in a traditional lime kilns have a higher ionic concentration in solution that can be attributed to a higher charge. Previous research conducted on these materials indicates that quicklime obtained by traditional procedure presented more charge, independently of the temperature reached, than the quicklime obtained by industrial kiln. On the other hand the calcination process of limestone modifies the surface free energy components of the rock; quicklime is more hydrophilic when produced in a traditional kiln [39].

4. Discussions

In this paper we analyze three different types of quicklimes originated in kilns with different production technology:

- A traditional lime kiln characterized by a slow calcination that favors the progressive heat transmission and CO_2 output. The selective arrangement of the limestone fragments in the kiln, according to size and distance to the heat source, allows a homogeneous cooking even though the temperatures inside the kilns are variable (between 750 and 1100 °C).
- Industrial limes kiln with reduced calcination time and temperatures around 900 °C, where the output of CO2 can be hindered due to the high rate of the calcination process.
- Finally a CaO of analytical purity calcined under controlled conditions; with a total calcination of limestone fragments, combining high temperatures and smaller particle sizes, which favor the formation of CaO crystals with rounded shapes and smooth surfaces.

The comparative study and its correlation with other CaO obtained in the laboratory from the same type of limestones allowed us to establish differences of interest. The importance of the type of limestone in the characteristics of the obtained CaO is confirmed, which can vary significantly the optimum calcination temperatures and produce sintering at temperatures below 1000 °C. At temperature range from 800 to 1000 °C there are important variations in the volume and distribution of the pore size, which is a function of the microtexture of the limestone, although it also highlights the incidence of temperature, pressure of CO_2, residence time in the kiln and size of the particles.

The physical properties of the CaO of traditional production may be related to the optimum calcination conditions, adapted to each type of limestone and kiln requirements. These aspects can be controlled by visual observations such as the emission of smoke, its color and the appearance of the calcined stone. The gradual and homogeneous calcination generates more porous CaO. Although the size and porosity of the CaO crystals are related to the initial limestone microtexture, these are modified during the calcination process. Under conditions of moderate CO_2 pressure (30%) the size of the CaO particles increases with the calcination time and temperature [26]. These conditions could be attributed to the traditional lime production technology, based on the nanotextural characteristics of the CaO observed in this type of kilns. In traditional lime kilns, although the calcination temperature in certain areas can reach 1100 °C (as is often the case in areas near the heat source), the high concentration of steam (higher in the area of combustion of wood), contributes to that the CaO structure does not collapse as expected, but on the contrary increases its porosity as occurs CaO(TL1).

In short periods of calcination and abrupt heating of the limestone, the pores are closed preventing the output of CO_2 to the outside, hindering the complete calcination of the limestone. The CaO crystals can grow rapidly but their size decreases with the calcination time and the reaction slows down since CO_2 desorption and structural transformations are hampered [26]. This could explain the textural characteristics observed in the CaO from the industrial kilns, smaller size and aggregation of CaO nanocrystals.

The microtextural characteristics of CaO(PL) indicate that the calcination has been complete and homogeneous. In this case the decomposition could have been controlled by the chemical reaction. The dominant mechanism at low CO_2 partial pressures for CaO crystal growth would be sintering of the nanocrystals by lattice diffusion which is promoted by an increase of temperature [26].

A correlation is established between CaO(TL1) and CaO(PL) in terms of surface area values, total pore volume (mesopores and micropores) and slaking kinetics, which result in a low exothermic reaction and few variations in electrical conductivity. This is explained by the greater volume of pores that allows faster access of water to the interior of the material and consequently the chemical reaction is less exothermic.

Correlations are established between CaO(IL) and CaO(PL) in terms of crystal size, and reaction kinetics, which result in rapid drop of pH and electrical conductivity. This is explained because the crystals size influences that the slaking reaction is more quickly.

Correlations are established between CaO(TL1) and CaO(TL2) in terms of larger crystal size, a slower slaking reaction, and more homogeneous pH values. This indicates that the conditions of calcination reached in traditional kilns affect the concentration of Ca^{+2} and OH^- ions in the solution and slower precipitation of $Ca(OH)_2$.

5. Conclusions

Based on the analysis of the results, the following conclusions are established:

- This paper shows the complexity of the calcination process of the limestone, although the temperature controls the process, the compositional and textural characteristics are important factors in the micro-textural evolution of the CaO. The calcination process of the limestones and the optimum calcination temperature depends of the porosity and crystalline structure original of the limestones.
- The importance of the traditional process of calcination of lime is indicated, since the control of visual indicators allows to establish the optimal calcination conditions for each type of stone as characteristics of the smoke (volume and color) and appearance of the calcined stone.
- The quicklimes calcined in traditional kilns are characterized by greater particle and pore size and greater volume of mesopores.
- The quicklimes with greater volume and size of pores allow faster access of water to the interior of the material and consequently the lime slaking reaction is less exothermic.
- The size of the particles CaO affects the rate of the lime slaking reaction, accelerating the reaction when the particles are smaller.

Conflict of interest

None declared.

Acknowledgements

We gratefully acknowledge the support of the institutions involved. This work was partially funded by University of Granada, University of Jaén, Research Group RNM349 of the Junta de Andalucía and Project -*Standardization of the use of lime for its application in conservation of Cultural Heritage*-. Andalusian Historical Heritage Institute. Spain (IAPH). Gordillo's Cal de Moron (Seville, Spain).

References

[1] J. Ashurst, F. Dimes, The cleaning and treatment of limestone by the lime method, Conserv. Build. Décor. Stone 2 (1990) 169–184.
[2] E.F. Hansen, C. Van Rodríguez-Navarro, K. Balen, Lime putties and mortars: Insights into fundamental properties, Studies Conserv. 53 (2008) 9–23.
[3] A. Mohammadinia, A. Arulrajah, H. Haghighi, S. Horpibulsuk, Effect of lime stabilization on the mechanical and micro-scaleproperties of recycled demolition materials, Sustainable Cities Soc. 30 (2017) 58–65.
[4] A. Arulrajah, A. Mohammadinia, I. Phummiphan, S. Horpibulsuk, W. Samingthong, Stabilization of recycled demolition aggregates by geopolymers comprising calcium carbide residue, fly ash and slag precursors, Constr. Build. Mater. 114 (2016) 864–873.
[5] F. García-Labiano, A. Abad, L.F. de Diego, P. Gayán, J. Adánez, Calcination of calcium –based sorbents at pressure in a broad range of CO_2 concentrations, Chem. Eng. Sci. 57 (2002) 2381–2393.
[6] R.S. Boynton, Chemistry and Technology of Lime and Limestone, Wiley, Inter science, London, 1980, p. 56.
[7] S. Dash, M. Kamruddin, P.K. Ajikumar, A.K. Tyagi, B. Raj, Nanocrystalline and metastable phase formation in vacuum thermal decomposition of calcium carbonate, Thermochim. Acta 363 (2000) 129–135.
[8] D.T. Beruto, R. Vecchiattini, M. Giordani, Solid products and rate-limiting step in the thermal half decomposition of natural dolomite in a CO2 (g) atmosphere, Thermochim. Acta 405 (2003) 183–194.
[9] D.T. Beruto, R. Vecchiattini, M. Giordani, Effect of mixtures of H_2O (g) and CO_2 (g) on the thermal half decomposition of dolomite natural stone in high CO_2 pressure regime, Thermochim. Acta 404 (2003) 25–33.
[10] C.N. Satterfield, F. Feakes, Kinetics of the thermal decomposition of calcium carbonate, AIChE J. 5 (1959) 115–122.
[11] F. Alou, V. Fulan, Materiaux de construcción. Chapitre II. Liants mineraux. Lausanne, Ecole Polytecnhnique Fedreale, 1989, Lausance.
[12] F. Schwarzkopf, Tecnología de la calcinación, 1978, pp. 66–68.
[13] R.H. Borgwardt, N.F. Roache, K.R. Bruce, Method for variation of grain size in studies of gas-solid reactions involving CaO, Ind. Eng. ing. Chem. Fundam. 25 (1986) 165–169.
[14] F. Rubiera, B.A. Faurtes, J.J. Pis, V. Artos, G. Marban, Changes in textural properties of limestone and dolomite during calcination, Thermochim. Acta 179 (1991) 125–134.
[15] E. Kristóf-Makó, A.Z. Juhász, The effect of mechanical treatment on the crystal structure and thermal decomposition of dolomite, Thermochim. Acta 342 (1999) 105.
[16] B.R. Stanmore, P. Gilot, Review-calcination and carbonation of limestone during thermal cycling for CO2 sequestration, Fuel Process. Technol. 86 (2005) 1707–1743.
[17] H. Shi, Y. Zhao, Effects of tempertures on the hidration characteristics of free lime, Cem. Concr. 32 (2002) 798–1793.
[18] C. Rodríguez-Navarro, E. Ruiz-Agudo, A.A. Luque, Huertas M. Ortega, Thermal descomposition of calcite: mechanism of formation and textural evolution of CaO monocrystals, Am. Mineral. 94 (4) (2009) 578–593.
[19] K. Kudlacz, C. Rodríguez Navarro, The mechanism of vapor phase hydration of calcium oxide: implications for CO2 capture, Environ. Sci. Technol. 21 (2014) 12411–12418.
[20] N.A. Rashidi, M. Mohamed, S. Yusup, A study of calcination and carbonation of cockle shell, Eng. Technol. (2011) 818–823.
[21] P. Basu, B. Achayra, A. Dutta, Study of calcination-carbonation of calcium carbonate in different fluidizing mediums for chemical looping gasification in circulating fluidized beds, in: 10th International Conference on Circulating Fluidized Beds and Fluidization Technology, CFB, 10, 2011, pp. 5–2.
[22] N. Nordin, Z. Hamzah, O. Hashim, F.H. Kasim, R. Abdullah, Effect of temperature in calcination process of seashells, Malaysian J. Anal. Sci. 19 (1) (2015) 65–70.
[23] J.R. Ingraham, P. Marier, Kinetic studies on the thermal decomposition of calcium carbonate, Can. J. Chem. Eng. 41 (1963) 170–173.
[24] J.A. Murray, Summary of fundamental research on lime and application of results to commercial problems. Report of National lime Association, 1956, Washington, DC.
[25] P. Maina, Improvement of lime reactivity towards desulfurization by hydration agents, Chem Sci Trans. 2 (1) (2013) 147–159.
[26] J.M. Valverde, P.E. Sanchez-Jimenez, L.A. Perez-Maqueda, Limestone calcination nearby equilibrium: kinetics, CaO crystal 2 structure, sintering and reactivit, J. Phys. Chem. C 119 (4) (2015) 1623–1641.
[27] F. Ger Lobez, Manual de Construcción Civil. Badajoz, imprenta de Minerva Extreña, 1898.
[28] D. Sagredo, Medidas del romano o Vitrubio casa de Ivan Ayala, 1549, Toledo.

[29] P. Cataneo Senese, Quattro primi libri di architettura, Vinegia, in cas de figliuoli di Aldo, Ediccion facsímil. In The Gregg Press Incorporated, 1964, Holanda.
[30] L. Battista Alberti, De re Aedificatoria, Florencia, Appresso Lorenzo Torrentino Impresssor Ducale, edicion facsimile traducida por Javier Fresnillo Nuñez. Ediciones Akal, 1991, Madrid.
[31] A. León Battista, Los diez libros de Arquitectura. Madrid. Alonso Gómez, trad. Francisco Loçano, (1958) 476.
[32] S. Pavia, S. Carol, An investigation of roman mortar technology through the petrographic analysis of archaeological material, Constr. Build. Mater. 22 (2008) 1807–1811.
[33] M. Fontenay, Novísimo manual práctico de las construcciones rústicas ó guía para los habitantes del campo y los operarios en las construcciones rurales, por M. de Fontenay, 1858, Madrid: Calleja, López y Rivadeneyra editores.
[34] Garate Rojas I. Artes de la cal. Munillaleria, 2002, p. 415.
[35] F. Alou, V. Fulan, Materiaux de construcción. Chapitre II. Liants mineraux. Lausanne, Ecole Polytecnhnique Fedreale, 1989, Lausance.
[36] C.A. Jombert, Architecture moderno u lárt de bien bâtir pour toutes sortes de personnes tant pour les maisons des particuliers que pour les palais. Contenabt cinq traites Genova, Tomo I y II, 1973.
[37] K.E. Ochaeta Paz, Análisis de las curvas termogravimétricas (640 mm hg) para el estudio de la calcinación de tres calizas con diferente contenido de magnesio en función de la densidad utilizando el método ASTM C 188-95. Tesis Universidad de Guatemala, 2004, 93.
[38] J.M. Valverde, P.E. Sanchez-Jimenez, L.A. Perez-Maqueda, Relevant influence of limestone crystallinity on CO_2 capture in the Ca-looping technology at realistic calcination conditions, Environ. Sci. Technol. 48 (16) (2014) 9882–9889.
[39] Ortega E. Ontiveros, Ortega A. Ontiveros, J.A. Baca Moleón, E.M. Ruiz Agudo, Electrokinetic and thermodynamic characterization of lime-water interface: physical and rheological properties of lime mortar, Constr. Build. Mater.. 151 (2017) 809–818.
[40] P.C. Okonkwo, S.S. Adefila, Investigation of some factors that affect jakura limestone burning, African J. Pure Appl. Chem. 7 (8) (2013) 280–290.
[41] G. Carrera, M.La. Olivi, cal investigación, patrimonio y restauración, Fical (2014) 149–166.
[42] P.C. Espinosa, Manual de construcciones de albañilería, 1859, Madrid.
[43] J. Wuhrer, On the Reactivity of Lime from Different Kilns Systetems, National Lime Association, Washington, D. C., 1965.
[44] Cruz-Sanjulian J. Estudio geológico del sector Cañete la Real. Teba-Osuna (Cordilleras Béticas, región occidental). Tesis doctoral Universidad de Granada, n° 71. Secretariado de Pub. Universidad de Granada, XII, 1974, pp. 431.
[45] ASTM C110, Standard Test Methods for Physical Testing of Quicklime Hydrated Lime and Limestone, American Society for Testing and Materials, Philadelphia PA, 2016.
[46] R. Folk, Petrology of Sedimentary Rocks. Ed Hemphill's, Austin, 1968, 170.
[47] E. Flügel, Microfacies of Carbonate Rocks, Analysis, Interpretation and Application, Springer Heidelberg Dordrecht, New York, 2010, p. 929.
[48] P. Ortiz, E. Mayoral, M.A. Guerrero, E. Galán, Caracterización petrográfica y geoquímica de las calizas de La Sierra de Estepa (Sevilla) y evaluación de la calidad técnica como material de construcción, Estudios Geol. 51 (1995) 213–222.
[49] Y. Díaz, Producción de la cal en hornos de Cuba. Experiencia en Antillana de Acero, 2009, in: https://www.researchgate.net/publication/308417221.
[50] G.H. McClellan, J.L. Eades, The Textural Evolution of Limestone Calcines, in: The Reaction Parameters of Lime. ASTM Special Publication 472, American Society for Testing and Materials, Philadelphia, 1970, pp. 209–227.
[51] Y. Zhu, S. Wu, X. Wang, Nano CaO grain characteristics and growth model under calcination, Chem. Eng. J. 175 (2011) 512–518.
[52] A.F. Zozulya, I.D. Zaitsev, V.A. Telitchenko, V.A. Rkach, Study of the kinetics of lime hydration, Chem. Abstr. 97 (1980) 257.
[53] E.K. Ovechkin, L.M. Volova, A.E. Chernaya, Reaction rate of lime slaking with preparation of concentrated milk of lime, Chem. Abstr. 78 (1972) 283.
[54] I.M. Ritchie, X. Bing-an, The Kinetics of lime slaking, Hidrometallurgy 23 (1990) 377–396.
[55] H.G. Shin, H. Kim, Y.N. Kim, H.S. Lee, Effect of reactivity of quick lime on the properties of hydrated lime sorbent for SO2 removal, J. Mater. Sci. Technol. 25 (2009) 329–332.